16

F. Alroumi, *et al.*: Characterization of Control Rod Worths and Fuel Rod Power ...
Nuclear Technology & Radiation Protection: Year 2016, Vol. 31, No. 1, pp. 16-27

CHARACTERIZATION OF CONTROL ROD WORTHS AND FUEL ROD POWER PEAKING FACTORS IN THE UNIVERSITY OF UTAH TRIGA MARK I REACTOR

by

Fawaz ALROUMI, Donghoon KIM, Ryan SCHOW, and Tatjana JEVREMOVIC[*]

Nuclear Engineering Program, The University of Utah, Salt Lake City, Ut., USA

Control rod reactivity (worths) for the three control rods and fuel rod power peaking factors in the University of Utah research reactor (100 kW TRIGA Mark I) are characterized using the AGENT code system and the results described in this paper. These values are compared to the MCNP6 and existing experimental measurements. In addition, the eigenvalue, neutron spatial flux distributions and reaction rates are analyzed and discussed. The AGENT code system is widely benchmarked for various reactor types and complexities in their geometric arrangements of the assemblies and reactor core material distributions. Thus, it is used as a base methodology to evaluate neutronics variables of the research reactor at the University of Utah. With its much shorter computation time than MCNP6, AGENT provides agreement with the MCNP6 within a 0.5 % difference for the eigenvalue and a maximum difference of 10% in the power peaking factor values. Differential and integral control rod worths obtained by AGENT show well agreement with MCNP6 and the theoretical model. However, regulating the control rod worth is somewhat overestimated by both MCNP6 and AGENT models when compared to the experimental/theoretical values. In comparison to MCNP6, the total control rod worths and shutdown margin obtained with AGENT show better agreement to the experimental values.

Key words: AGENT, TRIGA, MCNP6, control rod worth, reactivity, criticality, power peaking factor

INTRODUCTION

The University of Utah TRIGA Mark I Reactor (UUTR) is a pool-type research reactor of hexagonal core geometry, licensed to operate at the maximum power of 100 kW. The UUTR is used for research and academic training and educational purposes. Experiments conducted at the UUTR mostly involve neutron activation analysis (NAA), a non-destructive analytical element analysis technique, as well as irradiation of materials and electronics devices.

The UUTR fuel is composed of uranium zirconium hydride (UZrH) which has a large prompt negative reactivity temperature coefficient and, hence, it is an inherently safe design. The core consists of 127 cylindrical channels for fuel elements, reflectors, moderator and control rods; the core configuration is shown in fig. 1. There is a total of 78 fuel rods, 12 graphite and heavy reflectors (12 each), and three (3) control rods. The control rods are made of boron carbide with aluminum cladding. The three control rods are: safety rod that is used for large reactivity insertion; shim control
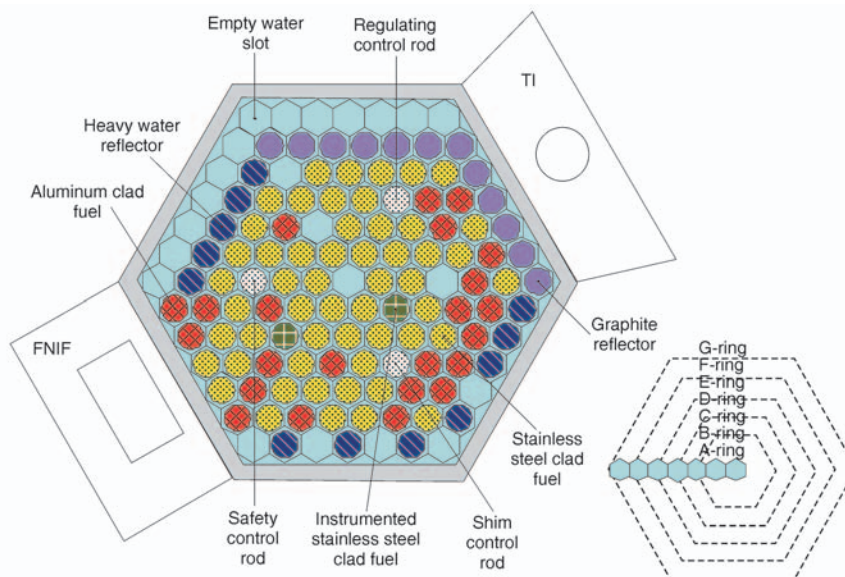
rod that is used for coarse power control; and regulating control rod that is used for fine reactivity change, such as to finely adjust the UUTR's power level. There are two irradiation ports located on the opposite ends of the reactor core: the fast neutron irradiation facility (FNIF) and the thermal irradiator (TI); they are used for various irradiation experiments. The TI port contains a heavy water moderator and has a high thermal to fast neutron flux density ratio. Furthermore, the TI port is for vial sized samples. The FNIF has a high fast neutron flux density and is made of lead, as it provides shielding from gamma rays. It has a larger volume than the TI port and, therefore, larger samples are placed in the FNIF for experiments.

The core excess reactivity is limited by technical specifications to 1.2 $\$$[*]. This limit assures the reactor can be shutdown at any time and the fuel temperature safety limit is not exceeded [1]. By definition, the shutdown margin is the amount of reactivity that is needed to make the reactor subcritical by the immediate insertion of control rods, with the exception of the most reactive control rod that remains fully withdrawn. The

---

[*] Corresponding author; e-mail: tatjana.jevremovic@utah.edu

[*] 1 $\$ = \beta_{\text{eff}}$ (the effective delayed neutron fraction)

F. Alroumi, *et al.*: Characterization of Control Rod Worths and Fuel Rod Power ...
Nuclear Technology & Radiation Protection: Year 2016, Vol. 31, No. 1, pp. 16-27

17

Figure 1. MCNP6 model of the UUTR core configuration [the fuel rings start from the center as A, going toward the core periphery where all three control rods are in ring D], [1]

UUTR shutdown margin is limited to 0.5 $ [1]. This value ensures the reactor can be brought to a subcritical state with the most reactive control rod fully withdrawn. Small research reactors are sensitive to reactivity insertions due to lower safety limits. Reactivity worths for each experiment are calculated. The single worth of a sample, and the total worth of all experiment samples, are limited to 1.0 $, and 1.2 $, respectively [1]. These limits are to ensure that the fuel safety limits are not exceeded. Furthermore, some experiments require high neutron flux density, and therefore, the reactor is then operated at the power level of 90 kW. Positive reactivity from experiments may lead to exceeding the maximum power limit of 100 kW. Hence the importance of estimating the reactivity worths as accurately as achievable. In the past, feasibility studies involving power upgrade of the UUTR have been conducted; more specifically, the control rods, cooling system design, and the requirements were fully evaluated [2, 3]. Moreover, neutron and gamma flux density in the irradiation ports have also been assessed as detailed in [4].
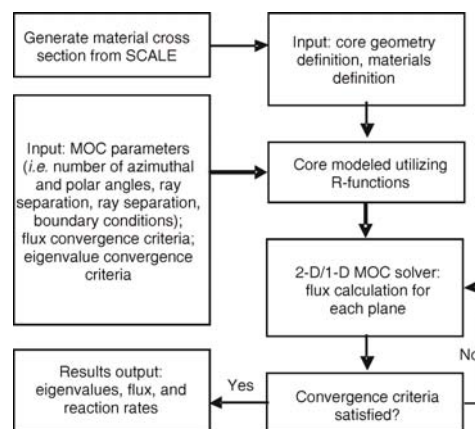
THEORETICAL BACKGROUND

AGENT methodology

Arbitrary geometry neutron transport (AGENT) is a deterministic neutron transport code that is based on the method of characteristics (MOC) and the theory of R-Functions [6-10]. The AGENT code system is widely benchmarked and in this case it is used to evaluate the control rod worths and power peaking factors in the UUTR, as well as the eigenvalue in its steady state operation, flux density distribution in the core, and the fission and absorption reaction rates. MCNP version 6 [11] is used for comparison with AGENT as well as with experimental values where appropriate.
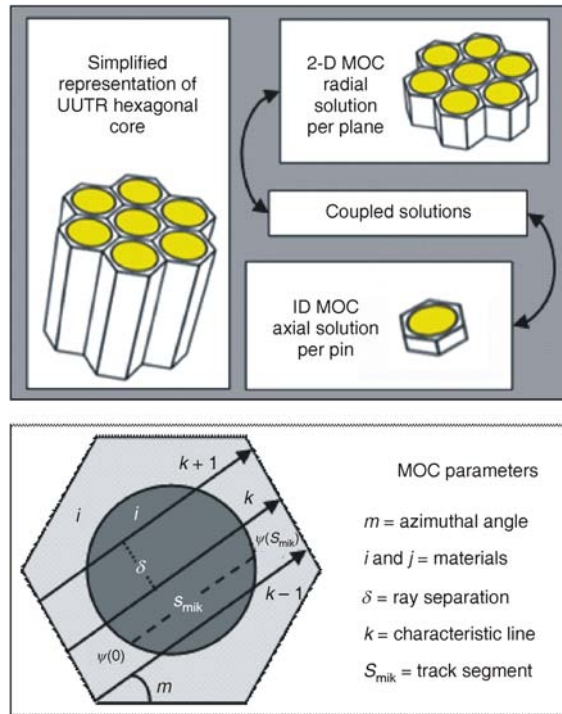
The 3-D modeling of a reactor's steady state with AGENT is based on 2-D/1-D coupled MOC equations through the neutron leakage term; the general flowchart of AGENT methodology is depicted in fig. 2. In the AGENT methodology, the reactor core is divided into 2-D radial planes and, therefore, a radial solution is obtained for each core plane configuration. A 1-D axial solution is then obtained for each pin region [8]. Figure 3 depicts the 2-D-1-D coupling and shows basic parameters of the MOC discretization applied in the AGENT methodology. The 3-D multigroup form of the Boltzmann neutron transport equation is given with

$$\hat{\Omega} \quad \psi^g(r,\hat{\Omega}) \quad \Sigma_t^g(r)\psi^g(r,\hat{\Omega}) \quad Q^g(r,\hat{\Omega}) \quad (1)$$

where, $\psi^g(r,\hat{\Omega})$ is the angular neutron flux density in energy group g, $\Sigma_t^g(r)$ is the total macroscopic scattering cross section for energy group g, and $Q^g(r,\hat{\Omega})$ is the multigroup neutron source term in energy group g, which is composed of isotropic fission and scattering terms

Figure 2. General 3-D AGENT methodology

18

F. Alroumi, *et al.*: Characterization of Control Rod Worths and Fuel Rod Power ...
Nuclear Technology & Radiation Protection: Year 2016, Vol. 31, No. 1, pp. 16-27

Figure 3. MOC coupled solutions of 2-D/1-D AGENT for the evaluation of UUTR

$$Q^g(\boldsymbol{r},\hat{\Omega}) = \frac{\chi^g}{4\pi k}\int_{4\pi}d\hat{\Omega}\sum_{g=1}^{G}\nu\Sigma_f^g(\boldsymbol{r})\psi^{g'}(\boldsymbol{r},\hat{\Omega}) + \int_{4\pi}d\hat{\Omega}\sum_{g=1}^{G}\Sigma_s^g(\boldsymbol{r},\hat{\Omega}\hat{\Omega})\psi^g(\boldsymbol{r},\hat{\Omega}) \qquad (2)$$

Equation (1) is integrated to obtain the characteristic form of the Boltzmann equation as follows:

$$\frac{d\psi^g(\boldsymbol{r_0}+s\hat{\Omega},\hat{\Omega})}{ds} = \Sigma_t^g(\boldsymbol{r_0}+s\hat{\Omega},\hat{\Omega})\psi^{\gamma}(\boldsymbol{r_0}+s\hat{\Omega},\hat{\Omega}) + Q^g(\boldsymbol{r_0}+s\hat{\Omega},\hat{\Omega}) \qquad (3)$$

where s is the track segment. Equation (3) is evaluated by analytical integration to express the outgoing angular neutron flux density along the characteristic lines (representing the neutron paths of a nuclear reactor in the 3-D space)

$$\psi_{m,i,k}^{g,out} = \psi_{m,i,k}^{g,in}e^{-\Sigma_t^{g,i}s_{m,i,k}} + \frac{Q^{g,i}}{\Sigma_t^{g,i}}(1-e^{-\Sigma_t^{g,i}s_{m,i,k}}) \qquad (4)$$

where $\psi_{m,i,k}^{g,out}$ is the outgoing angular neutron flux density of energy group g, at azimuthal angle m, in a material zone i, along characteristic line k; $\psi_{m,i,k}^{g,in}$ – the represents the incoming angular neutron flux density in energy group g, at azimuthal angle m, in material zone i, along characteristic line k. Thus, the change in angular neutron flux density is obtained by integration of eq. (4) to yield, [8]

$$\frac{d\psi_{m,i,k}^g}{ds_{m,i,k}} = \Sigma_t^g\psi_{m,i,k}^g + Q^{g,i} + LA_{m,i,k}^g \qquad (5)$$

where $d\psi_{m,i,k}^g/ds_{m,i,k}$ is the change in angular neutron flux density in energy group g, at azimuthal angle m, in material zone i, along characteristic line k, over the change in segment s. $\Sigma_t^g\psi_{m,i,k}^g$ represents the reaction rate in energy group g, at azimuthal angle m, in material zone i, along characteristic line k. The term $LA_{m,i,k}^g$ represents the axial neutron leakage in energy group g, at azimuthal angle m, in material zone i, along characteristic line k. Equation (5) thus represents the 2-D MOC solution per each radial plane later coupled with an axial leakage term. Therefore, the 1-D solution to each pin cell is expressed with

$$\frac{d\psi_{m,k,n}^g}{ds_{m,k,n}} = \Sigma_t^g\psi_{m,k,n}^g + Q^{g,n} + LR_{m,k,n}^g \qquad (6)$$

where $d\psi_{m,k,n}^g/ds_{m,k,n}$ is the change in angular neutron flux density in energy group g, at azimuthal angle m, in material zone i, along characteristic line k, at polar angle n, over the change in the segment; $\Sigma_t^g\psi_{m,k,n}^g$ – the reaction rate in energy group g, at azimuthal angle m, along characteristic line k; $Q_{g,n}$ – the pin-cell source term in energy group g at polar angle n; $LR_{m,k,n}^g$ – the radial neutron leakage term in energy group g, at azimuthal angle m, along characteristic line k, at polar angle n.

Rod worth and core reactivity calculations

Safety, shim and regulating rods are the three control rods of the UUTR reactor. The rod worth was determined using AGENT and MCNP6 for various cases by withdrawing each rod in increments of 5 %, with respect to its length, while the other two rods remained fully submerged. For every increment of a control rod withdrawal, positive reactivity is inserted into the core that is calculated with [12]

$$\rho = \frac{1-k_{\text{eff}}}{k_{\text{eff}}} \qquad (7)$$

The differential control rod worth represents a change in rod reactivity per rod unit length. Each control rod has a different reactivity worth and exposure to neutron flux density based on its location in the core. The differential control rod worth trend generally follows the neutron flux density profile in the core and, hence, the greatest reactivity effect is at the core center or, in other words, at 50 % of its rod withdrawal. These trends are estimated by taking into account the difference in reactivity between two subsequent rod positions divided by the amount of rod movement (unit length of rod withdrawal)[12], as follows

$$\frac{\rho_2-\rho_1}{\text{unit length}} = \frac{\dfrac{k_{\text{eff}_2}-k_{\text{eff}_1}}{k_{\text{eff}_2}k_{\text{eff}_1}}}{\text{unit length}} \qquad (8)$$

The integral control rod worth represents the total reactivity worth at a particular control rod position.

It is, therefore, a summation of the differential reactivity worths between a fully submerged and fully withdrawn control rod. The integral rod worth trend follows the "*s*" shape with a slope of the curve greatest at the core center (*i. e.*, 50 % control rod withdrawal), due to the highest neutron flux density being at that location in the reactor core.

Control rod worths are determined using a theoretical model as well and are, therefore, compared to the AGENT and MCNP6 models[12, 13] as follows

$$\rho_{\text{theo}} = A\sin^2\left[\frac{\pi(\%\text{out})}{2}\right]\beta_{\text{eff}} \quad (9)$$

where A is the respective total control rod worth (experimental data provided from UUTR operations log books), % out represents the percentage of control rod withdrawn, and β_{eff} – the effective delayed neutron fraction that is in the UUTR, estimated to be equal to 0.007.

The shutdown margin is defined as the amount of reactivity needed to make a reactor subcritical by the immediate insertion of control rods (the UUTR's shim and regulating rods), with the exception of the most reactive control rod fully withdrawn (the UUTR's safety rod) [1]

$$\rho_{\text{SDM}}(\$) = \frac{\frac{1-k_{\text{eff}_{\text{SO}}}}{k_{\text{eff}_{\text{SO}}}}}{\beta_{\text{eff}}} \quad (10)$$

where $\rho_{\text{SDM}}(\$)$ is the shutdown margin expressed in the unit of $, and $k_{\text{eff}_{\text{SO}}}$ represents the effective multiplication factor with the safety rod fully withdrawn, which is obtained from both AGENT and MCNP6 models.

Another important parameter in a research reactor is its excess reactivity, which compensates for fuel burn-up and negative reactivity due to inserted experiments. It is defined as the amount of reactivity available or in excess when the reactor is critical [1]

$$\rho_{\text{ER}}(\$) = \frac{\frac{k_{\text{eff}_{\text{c}}}-1}{k_{\text{eff}_{\text{c}}}}}{\beta_{\text{eff}}} \quad (11)$$

where $k_{\text{eff}_{\text{c}}}$ is the calculated eigenvalue with all control rods fully withdrawn.

Power peaking factors

Power peaking factors are one of the most important parameters in reactor core neutronics assessments and analysis. The power generated and released by each individual fuel rod relative to other fuel rods within the same fuel core section (in the case of UUTR, the so called ring) and the core average, resemble the fast flux density profile of the core. Knowledge of power distribution in the core provides insights into fuel performance and the rate of burn-up. AGENT cal-

culates the power per pin per each plane, and thus, the total power per pin is obtained with

$$P_{Fr_j} = \sum_{i=1}^{n} Pz_i \quad (12)$$

where P_{Fr_j} is the power released per fuel rod j, Pz_i – the local power in fuel rod i per plane z, and n – the total number of planes in the UUTR core. Therefore, the average power in the core is calculated [15]

$$P_{\text{avg}} = \frac{\sum_{j=1}^{N} P_{Fr_j}}{N} \quad (13)$$

where N represents the number of fuel rods in the core. Thus, the power peaking factor is determined by dividing the fuel rod power with the average reactor core power [15], as follows

$$P_{\text{PF}} = \frac{P_{Fr_j}}{P_{\text{avg}}} \quad (14)$$

For benchmark purposes, power distribution is also calculated using the F7 tally card in the MCNP6 model of the UUTR. The UUTR power level of 100 kW with 200 MeV per fission are assumed in determining the power peaking factors for the UUTR core.

AGENT and MCNP6 simulation parameters in assessing the UUTR's control rod worths and power peaking factors

AGENT and MCNP6 UUTR's simulation parameters are provided in tab. 1. Increasing the number of azimuthal angles and decreasing the size of ray separation in the AGENT model of the UUTR will increase the accuracy and CPU time. Therefore, MOC resolution parameters in the AGENT model of the UUTR are optimized in regard to the accuracy of CPU time, thus including 24 azimuthal angles and a ray separation of 0.05 cm. Furthermore, the geometrical submeshing pattern includes six triangular zones per hexagonal fuel rod. Due to the nature of the MOC solution, neutron flux density is constant in a submeshed

Table 1. AGENT and MCNP6 simulation parameters for the UUTR full 3-D core model

Parameter	AGENT	MCNP6
Number of azimuthal angels	24	n. a.
Number of polar angles and scheme	2, Leonard-McDaniel	n. a.
Ray separation [cm]	0.05	n. a.
Number of boundary edges per core face	264	n. a.
Geometry submeshing	6 triangles per hexagonal fuel rod	n. a.
Flux and eigenvalue iteration margins	10^{-5} and 10^{-6}	n. a.
Number of source particles / Total cycles (skipped cycles)	n. a.	1 million / 600 (150)
Initial eigenvalue	1.0	1.0

20

F. Alroumi, *et al.*: Characterization of Control Rod Worths and Fuel Rod Power ...
Nuclear Technology & Radiation Protection: Year 2016, Vol. 31, No. 1, pp. 16-27

material region, so regions are divided into as small zones as reasonably achievable. In general, in the MOC approach, decreasing the size of the zones will increase the accuracy of the solution. The flux and eigenvalue calculation are dependent on convergence criteria; these are selected to be 10^{-5} and 10^{-6} for the flux and eigenvalue values, respectively. The iteration will complete if the relative difference between the two iterations are less than or equal to the convergence limits, or a user-defined maximum number of iterations is reached. In the MCNP6 model, a total of 100 million neutrons and 600 cycles are used, resulting in the eigenvalue with a standard deviation of 10^{-4}.

UUTR control rod worth values

UUTR technical specifications require that the reactivity worth of each control rod must be determined semi-annually. This assures that the core remains safely loaded and the reactor operators know the reactivity effects of the control rods. Control rod worth in the UUTR is measured experimentally, using the control rod-drop method. The control rod-drop method utilizes an analog signal from the reactor linear power channel *vs.* time for a reactor's power trace. This method requires that the reactor power be kept at a constant level so that spurious noise is at a minimum and the fuel temperature remains ambient. At low reactor power levels, spurious noise may cause errors in control rod worth determination. At high power levels, fuel temperature effects are factored into reactivity calculations. High power operations should not have occurred in the run prior to performing the procedure. Such a procedure starts by dropping the regulator control rod from the fully withdrawn position while the UUTR core is critical at approximately 1 kW. Then, while leaving the regulating control rod inserted, the reactor is brought to critical condition by further withdrawing the shim control rod. After the reactor is allowed to stabilize at 1 kW, the shim control rod is dropped into the UUTR core. The shim control rod position must be noted at the time of its drop. Next, the UUTR core is, again, brought critical with the shim control rod and the safety control rod is dropped from the fully with drawn position at 1 kW.

The equations used for the analysis of the rod-drop method are space-independent reactor kinetic equations

$$\frac{\mathrm{d}\phi(t)}{\mathrm{d}t} = \frac{1-\beta}{\ell}k_{\text{ex}}(t)\phi(t)$$
$$-\frac{\beta}{\ell}\phi(t) + \sum_{i=1}^{6}\lambda_i C_i(t) \qquad (15)$$

$$\frac{\mathrm{d}C_i(t)}{\mathrm{d}t} = \frac{\beta}{\ell}a_i[1-k_{\text{ex}}(t)]\phi(t) - \lambda_i C_i(t) \quad (16)$$

where i is the delayed neutron group ($i = 1$ to 6), t – the time after disturbance of steady-state condition [s], β – the total effective delayed neutron fraction, ℓ = prompt neutron lifetime [s], $k_{\text{ex}}(t)$ – the time-dependent excess reactivity [$\Delta k/k$], $\phi(t)$ – the time-dependent neutron flux [$\text{cm}^{-2}\text{s}^{-1}$], λ_i – the precursor decay constant [s^{-1}], $C_i(t)$ – the time-dependent concentration of the precursor of the ith group of delayed neutrons [nuclei per cm^3], and a_i – the fraction of the total effective delayed neutron fraction in the ith group.

Equations (15) and (16) are then combined to obtain a relationship between the time-dependent excess reactivity, $k_{\text{ex}}(t)$, and neutron flux, $\phi(t)$, by using the initial conditions which exist at criticality just before the rod is dropped. The initial conditions are

$$k_{\text{ex}}(0) = 0 \text{ and } \frac{\mathrm{d}C_i(0)}{\mathrm{d}t} = 0 \qquad (17)$$

These initial conditions relate to the assumption that at time zero excess reactivity is zero and the delayed neutron precursor concentrations are in equilibrium. The result obtained by using these initial conditions combined with eqs. (15) and (16) is the following integro-differential equation

$$\frac{1-\beta}{\beta}k_{\text{ex}}(t) = 1 - \frac{\ell}{\beta}\frac{1}{\phi(t)}\frac{\mathrm{d}\phi(t)}{\mathrm{d}t}$$
$$-\frac{\phi(0)}{\phi(t)}\sum_{i=1}^{6}a_i e^{-\lambda_i t}$$
$$-\frac{1}{\phi(t)}\sum_{i=1}^{6}a_i\lambda_i e^{-\lambda_i t}\int_0^t[1-k_{\text{ex}}(t')]\phi(t')e^{\lambda_i t'}\mathrm{d}t' \quad (18)$$

Equation (17) was put into difference form and programmed in FORTRAN to obtain reactivity, $k_{\text{eff}}(t)$, as a function of time after rod drop. The value of the integral was calculated by use of an iterative procedure that employs interpolation and extrapolation of the available information. Reactivity was converted from $\Delta k/k$ units to the unit of $, using the relationship of 1$ $= \beta_{\text{eff}}$. From this, it is possible to determine the worth of the various control rods in the UUTR.

EVALUATION OF THE UUTR EIGENVALUE, CONTROL ROD WORTHS AND POWER PEAKING FACTORS OBTAINED WITH AGENT AND MCNP6 IN COMPARISON TO EXPERIMENTAL DATA

Comparison of the UUTR eigenvalues calculated with AGENT and MCNP6

The UUTR core is modeled using the AGENT code system without taking into account the presence of FNIF and TI ports. In order to make an adequate comparison, the UUTR model, with and without the ports, is modeled using MCNP6. Furthermore, the

F. Alroumi, *et al.*: Characterization of Control Rod Worths and Fuel Rod Power ...
Nuclear Technology & Radiation Protection: Year 2016, Vol. 31, No. 1, pp. 16-27

21

Table 2. Comparison of the UUTR eigenvalues obtained with AGENT and MCNP6

Method	k_{eff} control rods in		Diff [%]	k_{eff} control rods out		Diff [%]
AGENT	0.97955		Ref	1.00597		Ref
MCNP6 w/ports	0.97606	0.00004	0.36	1.00654	0.00003	–0.06
MCNP6 w/o ports	0.97509	0.00004	0.46	1.00550	0.00004	+0.05
MCNP5 [2, 5]	–		–	1.00400	0.00004	+0.2

*Diff = 100 [k_{eff}(AGENT, Ref) – k_{eff}(MCNP6)]/k_{eff}(AGENT, Reff)

simulation models are developed for both a fully controlled and uncontrolled UUTR reactor core. A summary of the calculated eigenvalues is presented in tab. 2. The values also include the MCNP5 model of the UUTR per [2, 5], for comparison. The AGENT value is used as a reference. In both cases (of fully inserted and fully withdrawn control rods), the difference between the calculated eigenvalues of AGENT and MCNP6 is less than 1 %. In the case of control rods fully withdrawn, when the neutron flux is higher, the eigenvalues agree much more closely. Eigenvalues from MCNP6 simulations without ports show to be slightly lower then those with ports included. The TI port has heavy water reflectors and, therefore, the neutron leakage from the core increases when the ports are not included in the model, giving lower eigenvalues. However, the difference between the two MCNP6 models is small. MCNP5 and MCNP6 exhibit a minimal difference. Therefore, the MCNP6 model with ports (more detailed geometry) is used for control rod worth calculations.

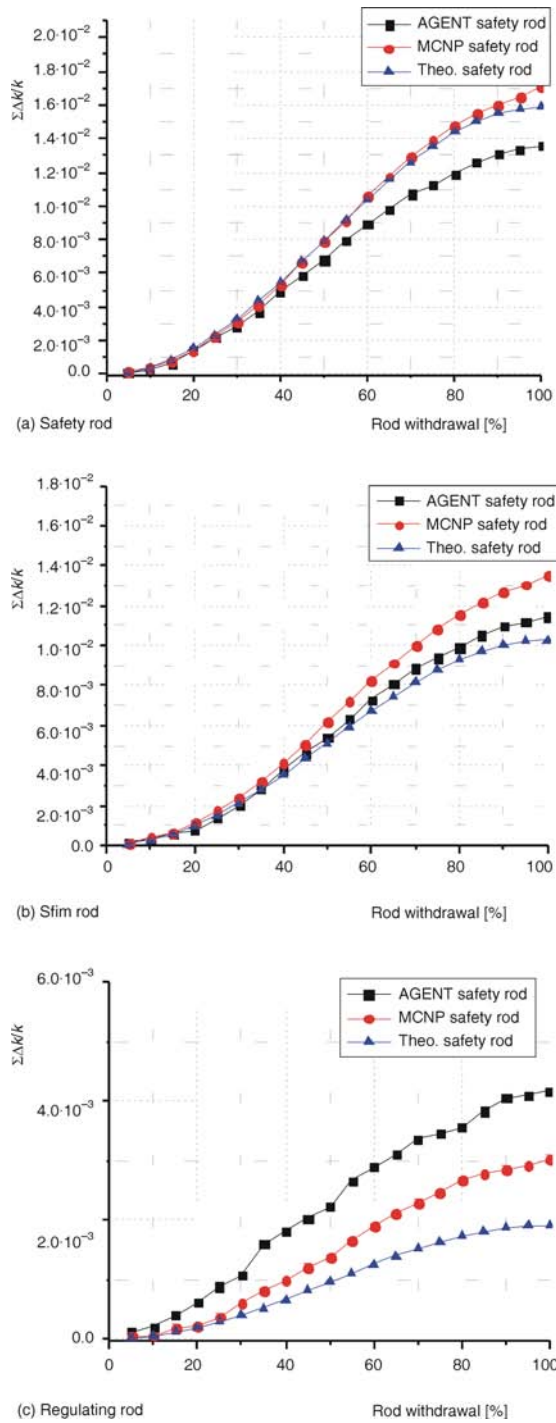## UUTR control rod worths and core reactivity values

The differential and integral control rod worth obtained from the AGENT and MCNP6 models (with FNIF and TI ports), in comparison to theoretical models (in the section *Rod worth and core reactivity calculations*), are shown in figs. 4 and 5, respectively. In the differential control rod worth trend shown in fig. 4, AGENT, MCNP6 and the theoretical models, all agree on both the safety and shim control rods. However, for the regulating control rod, both MCNP6 and AGENT give an overestimation compared to the theoretical model. The regulating control rod has the lowest reactivity worth, and hence, the flux density in that region is lower compared to the central region of the UUTR core. Therefore, calculations are more sensitive and better agreement is expected with reduced calculation uncertainties. In addition, the theoretical model is highly dependent on the value of β_{eff} which can be varied. As mentioned previously, the value of β_{eff} is equal to 0.007 in the theoretical model and the results may vary significantly with small changes to its value. However, results from the simulation do not utilize β_{eff}
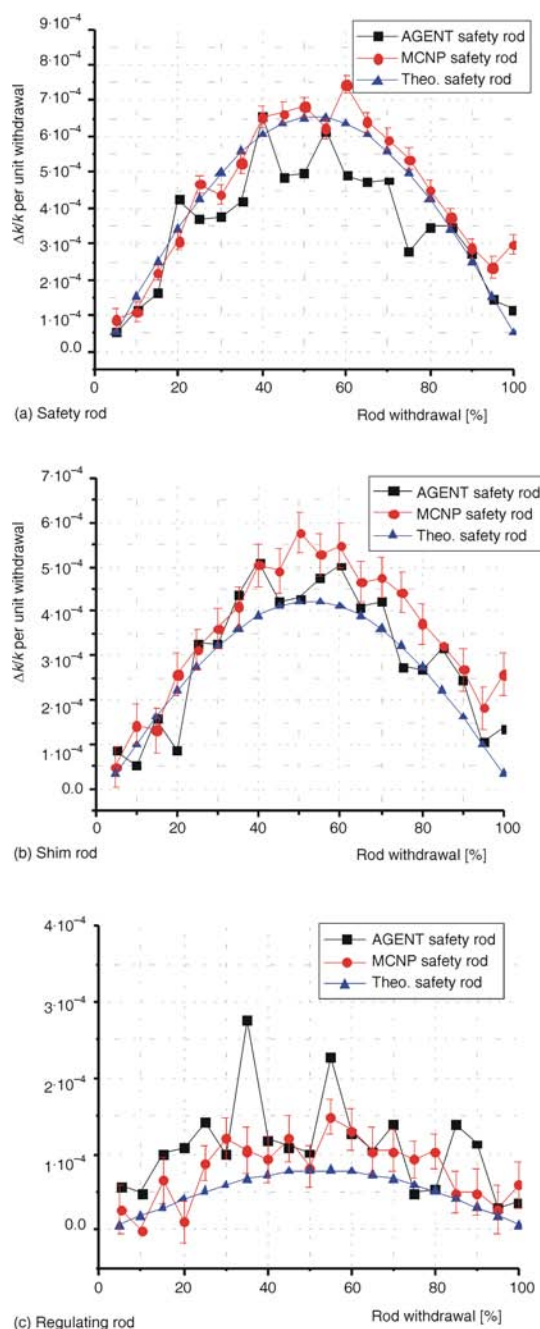
Figure 4. Comparison of the UUTR Differential Control Rod Worth determined with AGENT and MCNP6 with theoretical values [the safety control rod has the highest worth and the regulating control rod shows the least worth]

in providing the values for the integral and different control rod worth values eq. (2).

As can be seen from fig. 5, the AGENT calculated integral safety control rod worth shows some deviation, or underestimation, starting at the 50 % control rod withdrawal position. However, AGENT represents the shim control rod worth much accurately than MCNP6, as the values agree with the theoretical model. As for the regulating control rod, both MCNP6 and AGENT overestimate the control rod worth, as compared to the theoretical model.

22

F. Alroumi, *et al*.: Characterization of Control Rod Worths and Fuel Rod Power ...
Nuclear Technology & Radiation Protection: Year 2016, Vol. 31, No. 1, pp. 16-27

(a) Safety rod

(b) Sfim rod

(c) Regulating rod

Figure 5. Comparison of the UUTR integral control rod worth determined with AGENT and MCNP6 with

The regulating control rod is in a much lower flux density region and, therefore, the calculations are more sensitive. Table 3 shows a summary of the calculated control integral rod worths from simulations in comparison to experimental data. Values from AGENT simulations match the experimental and MCNP6 values for the shim and safety control rods. However, for the regulating control rod worth, both AGENT and MCNP6 overestimate the value somewhat. The regulating control rod has a much lower rod worth compared to the other three control rods, thus it

Table 3. Comparison of AGENT and MCNP6 control rod worths to experimental data

Method	AGENT	MCNP6 w/ports[*]		Experiment[**]
Shim control rod [$]	1.63	2.01	0.03	1.47
Safety control rod [$]	1.94	2.44	0.02	2.27
Regulating control rod [$]	0.60	0.44	0.02	0.27
Total worth [$]	4.17	4.89	0.04	4.01
Total worth difference [%]	3.8	17.9		Reference

[*] FNIF and TI ports, [**] UUTR semi-annual control rod calibrations (April 2015)

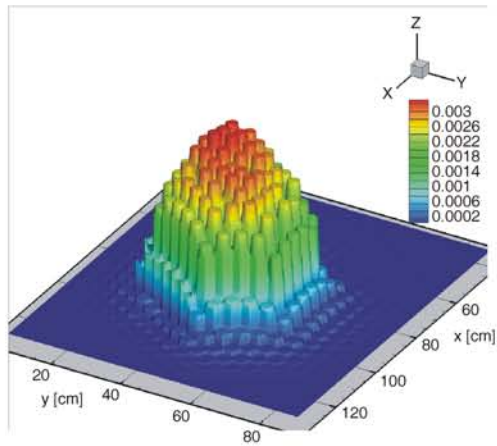**Table 4. Comparison of AGENT and MCNP6 shutdown margins to experimental values**

Method	Shutdown margin [$]		Difference [%]
AGENT	1.12		0.8
MCNP6 w/ports[*]	1.07	0.004	−4.0
Experiment[**]	1.11		Reference

[*] FNIF and TI ports, [***] UUTR operations log book (april 2015) [**] UUTR semi-annual control rod calibrations (april 2015)
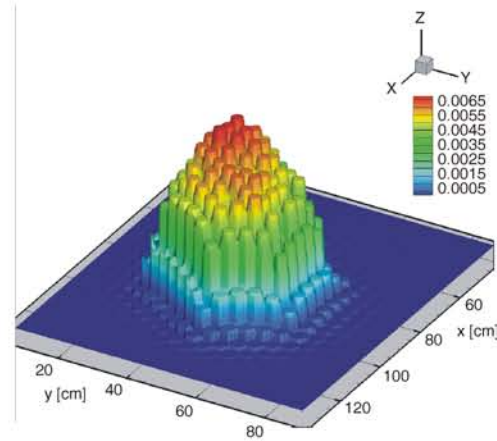
is exposed to a much lower neutron flux density. The regulating control rod worth has shown fluctuations in values (as can be seen in fig. 4) determined from simulations between each increment of rod withdrawal. Both simulation codes have overestimated the total worth for the regulating control rod. However, when comparing the total worth of all control rods, the AGENT value matches the experiment total rod worth much closer than that obtained with MCNP6. Table 4 shows the calculated shutdown margin in comparison to the experimental values. Both simulations match the experiment, but AGENT matches much more closely with a difference of just 0.8 %.

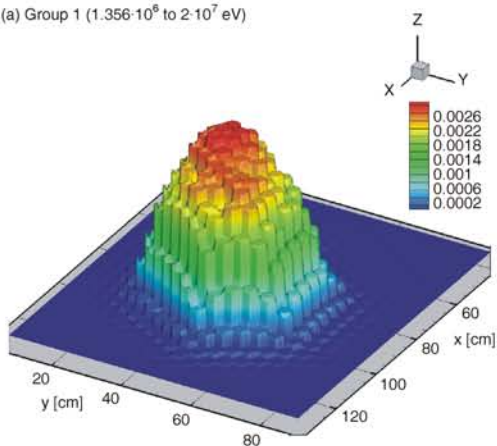**UUTR flux density distribution, reaction rates and power distribution**

Figures 6 to 9 show the flux density fission and absorptions rates distributions for an uncontrolled UUTR core, obtained with the AGENT model; the data are plotted using TECHPLOT 360 (Techplot Inc.) [16]. In figs. 6 and 7, the fast neutron flux density (energy group 1: $1.356 \cdot 10^6$ to $2 \cdot 10^7$ eV) shows the highest value to be in the central region of the UUTR core. As for the thermal neutron flux density (group 7: 10^{-5} to 0.125 eV), the highest flux density values peak at specific locations in the core. These locations are empty fuel rod positions, or slots, filled with water. Furthermore, the fast neutron flux density at the boundaries is significantly low, due to neutron leakage. Whereas in energy group 7, the thermal neutrons are not completely lost, because there are graphite and heavy water reflectors at the outer boundaries of the UUTR core.
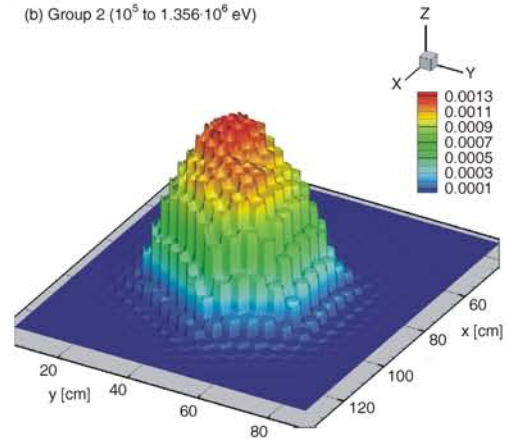
F. Alroumi, *et al*.: Characterization of Control Rod Worths and Fuel Rod Power ...
Nuclear Technology & Radiation Protection: Year 2016, Vol. 31, No. 1, pp. 16-27
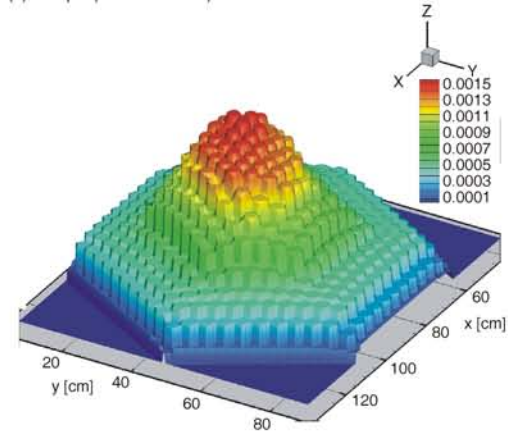
23

(a) Group 1 (1.356·10⁶ to 2·10⁷ eV)
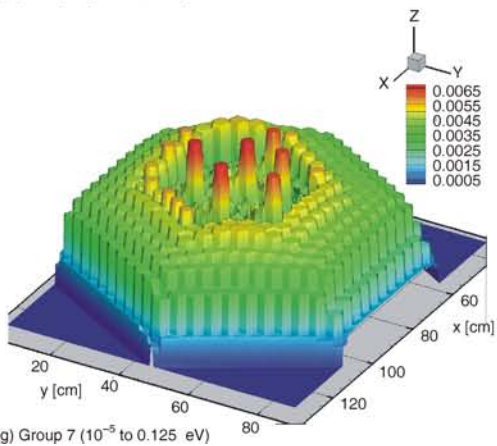
(b) Group 2 (10⁵ to 1.356·10⁶ eV)

(c) Group 3 (5.5·10¹ to 10⁵ eV)

(d) Group 4 (4 to 5.5·10¹ eV)
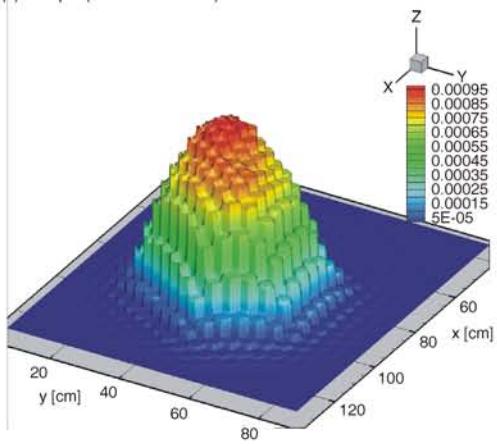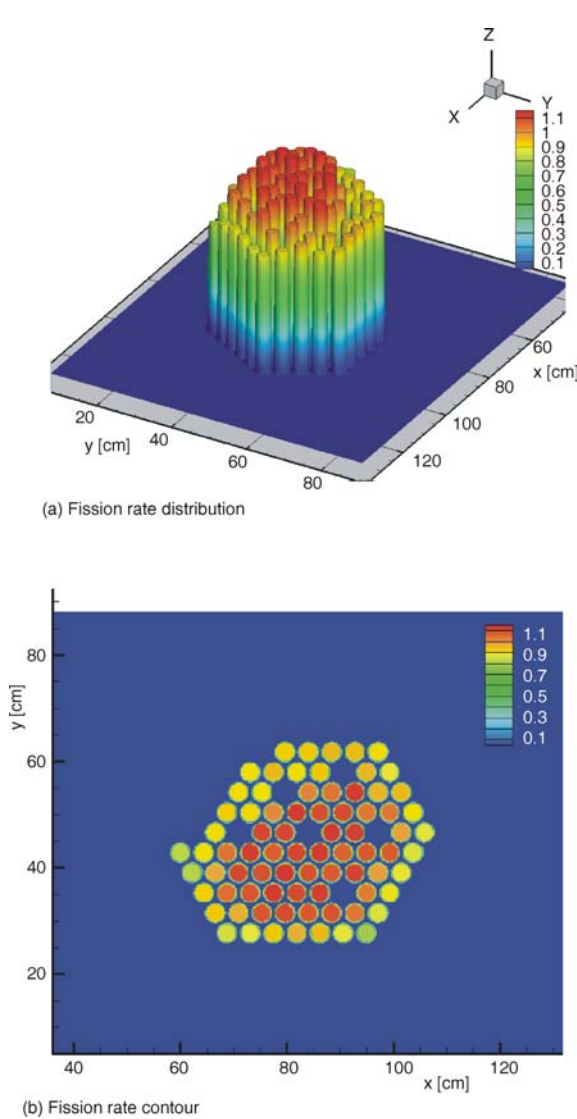
(e) Group 5 (0.625 to 4 eV)

(f) Group 6 (0.125 to 0.625 eV)

(g) Group 7 (10⁻⁵ to 0.125 eV)

Figure 6. AGENT UUTR flux density distribution, for seven energy groups (groups 1-2 are in the fast region, groups 3-4 in the resonance region, and groups 5-7 in the thermal region)

24

F. Alroumi, *et al*.: Characterization of Control Rod Worths and Fuel Rod Power ...
Nuclear Technology & Radiation Protection: Year 2016, Vol. 31, No. 1, pp. 16-27

(a) Group 1 (1.356·10⁶ to 2·10⁷ eV) x [cm]

(b) Group 2 (10⁵ ~ 1.35·10⁶ eV) x [cm]

(c) Group 3 (5.5·10¹ to 10⁵ eV) x [cm]

(d) Group 4 (4 to 5.5·10¹ eV) x [cm]

(e) Group 5 (0.625 to 4 eV) x [cm]

(f) Group 6 (0.125 to 0.625 eV) x [cm]

(g) Group 7 (10⁻⁵ to 0.125 eV) x [cm]
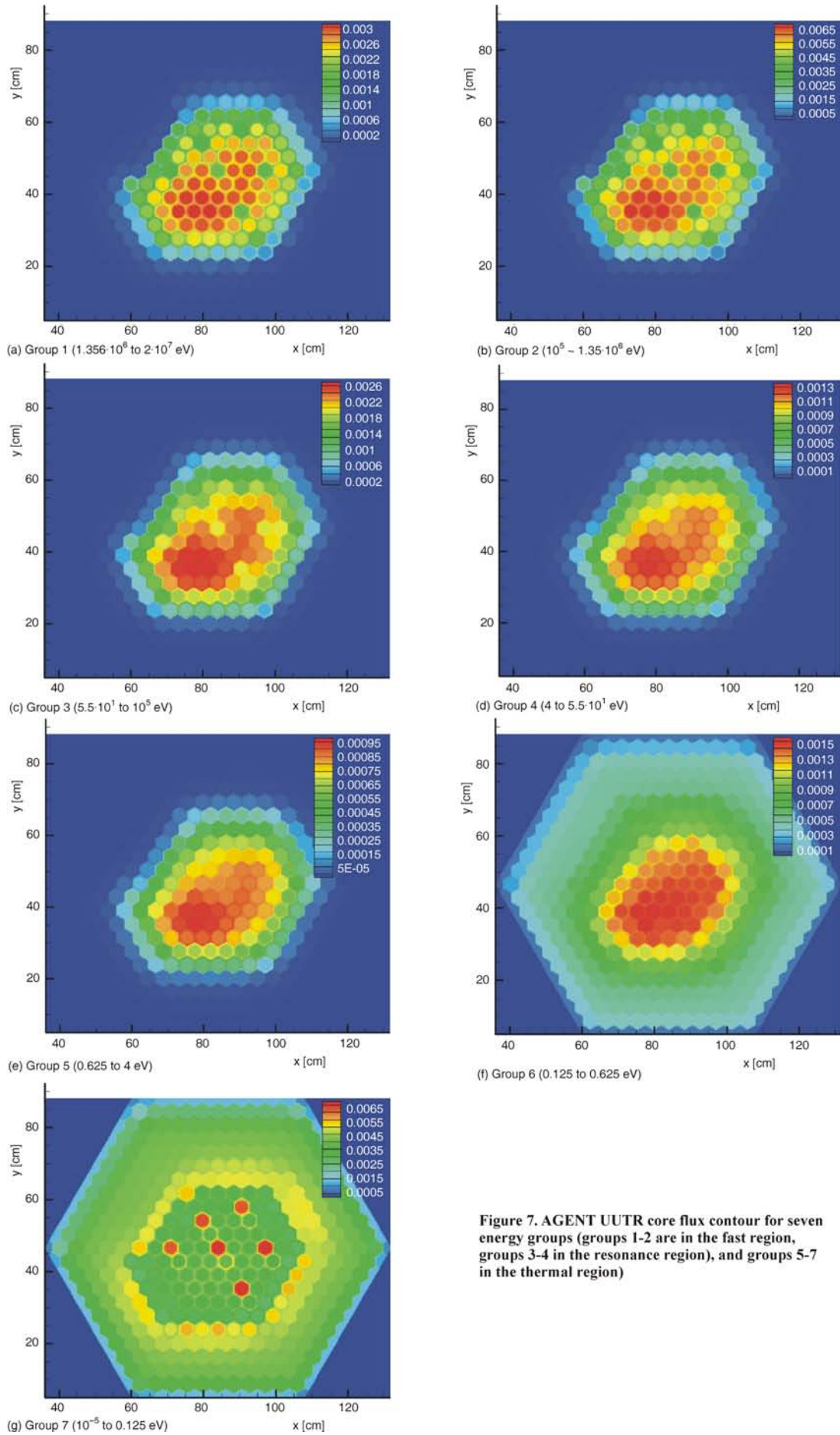
Figure 7. AGENT UUTR core flux contour for seven energy groups (groups 1-2 are in the fast region, groups 3-4 in the resonance region), and groups 5-7 in the thermal region)

F. Alroumi, *et al*.: Characterization of Control Rod Worths and Fuel Rod Power ...
Nuclear Technology & Radiation Protection: Year 2016, Vol. 31, No. 1, pp. 16-27

25

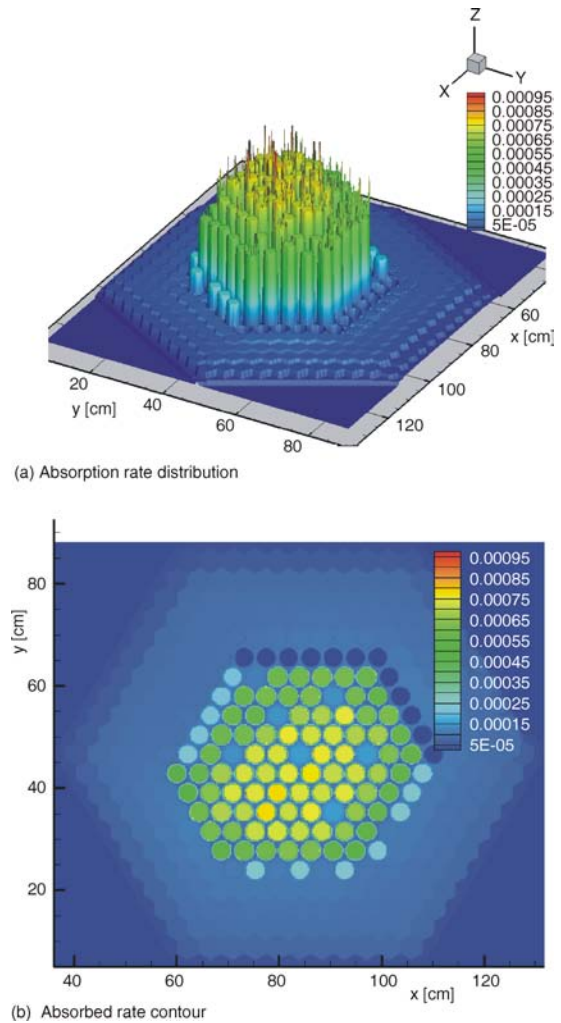(a) Fission rate distribution

(b) Fission rate contour

Figure 8. AGENT UUTR core; (a) fission rate distribution and (b) fission rate contour (the rate is highest at the center of the UUTR core, analogous to fast neutron flux density)

Figures 8 and 9 illustrate the fission and absorption rates spatial distributions in the UUTR core. From fig. 8, it can be seen that the fission reaction rates distribution has a similar profile to the fast neutron flux density distribution in the core.

Table 5 shows the calculated power peaking factors from MCNP6 and AGENT simulations. AGENT values are in well agreement with the MCNP6, with the highest difference of ~10 %. The highest peaking factor is in the F ring, while the lowest is in the B ring (fig. 1). Fuel rods with the highest burn-up are located in the core center, and the lowest fuel burn-up rods (almost fresh fuel) are located in the outer core rings. This arrangement is to ensure a uniform flux density and power distribution in the core.

Figure 10 shows the UUTR power peaking factor distribution per each fuel rod per each core ring. The trend shows AGENT and MCNP6 values, with and without the FNIF and TI ports. Based on these re-

(a) Absorption rate distribution

(b) Absorbed rate contour

Figure 9. AGENT UUTR core; (a) absorption rate distribution and (b) absorption rate contour (absorption rate is uniformly distributed throughout the UUTR core)
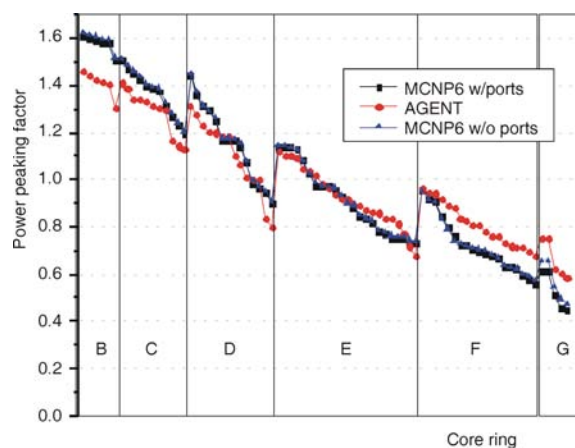
Figure 10. Comparisons of the UUTR power peaking factors obtained with AGENT and MCNP6 models

sults, it can be concluded that the FNIF and TI ports have pretty negligible effects on the power profile in the core. The AGENT power peaking factors show slight deviation from the MCNP6 values, more specifically, in the B, F, and G rings. Possible reasons for this deviation could be due to the deterministic nature of

26

F. Alroumi, *et al.*: Characterization of Control Rod Worths and Fuel Rod Power ...
Nuclear Technology & Radiation Protection: Year 2016, Vol. 31, No. 1, pp. 16-27

Table 5. Comparison of calculated power peaking factors

Ring	Number of fuel rods	P_{max}/P_{avg} (MCNP6)	P_{max}/P_{avg} (AGENT)	Difference[*] [%]
B	6	1.02	1.04	–2.0
C	11	1.10	1.10	0.0
D	14	1.24	1.19	4.0
E	23	1.25	1.22	2.4
F	19	1.32	1.19	9.9
G	5	1.16	1.14	1.7
Total	78	1.61	1.46	9.3

[*]Difference = $[1 - (P_{max}/P_{avg}$ AGENT$)/(P_{max}/P_{avg}$ MCNP6$)]$ 100 %

the code, and of the approximations, such as the number of energy groups. As for the stochastic nature of MCNP6, the associated uncertainties provide a calculation error that has to be considered. However, to properly investigate the deviation between simulation codes, experimental values must be determined in order to provide a better insight into the exact power peaking factors and their agreement with the simulation codes.

CONCLUSIONS

The UUTR core parameters such as eigenvalue, neutron flux density, reaction rates, control rod worths, and power peaking factors are characterized using the state-of-the-art codes, AGENT and MCNP6. The eigenvalue results from both codes are in well agreement, with the highest difference being less than 0.5 %. The differential and integral rod worth values obtained from AGENT and MCNP6 are also compared to a theoretical model. As for differential rod worth values, AGENT provides values highly comparable to the theoretical model and MCNP6. However, regarding the regulating control rod, there is a slight deviation between the AGENT and MCNP6 results. This is due to the low neutron flux density region that increases the sensitivity of the calculations. Both the said sensitivity and overestimation are reflected in the integral rod worth values. In addition, the agreement of the total rod worth and shutdown margin confirm the high accuracy of AGENT. The power peaking between the two codes shows good agreement, with a degree of deviation mostly in the B, F, and G rings.

ACKNOWLEDGEMENTS

The authors wish to thank H. Hernandez-Noyola and V. Vijay for their contribution and efforts in the development of the AGENT code system.

AUTHORS' CONTRIBUTIONS

F. Alroumi aplied MCNP and AGENT codes simulations of the UUTR to control rod worth calculations, power peaking factor calculations, generated the flux and reaction rates' plots.

D. Kim provided help with AGENT simulations and in analyzing the results. Also contributed to the

flux and reaction rates' plots and interpretation of the final values.

R. Schow wrote the section *UUTR control rod worth values* of the paper and provided help with comparing results of the simulations with the experimental data.

T. Jevremovic initiated this study and guided the authors to study completion, checked the results and provided a guiding to the analysis as summarized in this paper.

REFERENCES

[1] ***, University of Utah – Submission of Safety Analysis Report, Technical Specifications and Responses to NRC RAIs. 2010, Document #ML10321004

[2] Cutic, A., Choe, D., Jevremovic, T., Feasibility Study of the University of Utah TRIGA Reactor Power Upgrade, Part I: Neutronics-Based Study in Respect to Control Rod System Requirements and Design, *Nucl Technol Radiat, 28* (2013), 2, pp. 109-117

[3] Babitz, P., Choe, D., Jevremovic, T., Feasibility Study of the University of Utah Triga Reactor Power Up Grade Part II: Thermohydraulics and Heat Transfer Study in Respect to Cooling System Requirements and Design, *Nucl Technol Radiat, 28* (2013), 4, pp. 352-361

[4] Noble, B., Choe, D., Jevremovic, T., Experimental and MCNP5 Based Evaluation of Neutron and Gamma Flux in the Irradiation Ports of the University of Utah Research Reactors, *Nucl Technol Radiat, 27* (2012), 3, pp. 222-228

[5] ***, X-5 Monte Carlo Team, MCNP – Version 5, Vol I: Overview and Theory, LA-UR-03-1987, 2003

[6] Shaphiro, V., Real Functions for Presentation of Rigid Solids, *Computer Aided Geomtric Design, 11* (1994), 2, pp. 153-175 http://dx.doi.org/10.1016/0167-8396(94)90030-2

[7] Rvachev, V. L., Theory of R-Functions and Some Applications, Naukova Dumka, Ukraine, 1982

[8] Hernandez, H., *et al.*, Visual Numerical Steering in 3-D AGENT Code System for Advanced Nuclear Reactor Modeling and Design, Annals of Nuclear Energy, 55 (2013), May, pp. 248-257 http://dx.doi.org/10.1016/j.anucene.2012.12.008

[9] Hursin, M., Jevremovic, T., AGENT Code – Neutron Transport Benchmark Example and Extension to 3-D Lattice Geometry, *Nucl Technol Radiat., 20* (2005), 1, pp. 10-16

[10] Hursin, M., Xiao, S., Jevremovic, T., Synergism of the Method of Characteristics, R-Functions and Diffusion Solution for Accurate Representation of 3-D Neutron Interactions in Research Reactors Using the AGENT Code System, *Annals of Nuclear Energy, 33* (2006), 13, pp. 1116-1133

[11] Goorley, T., *et al.*, Initial MCNP6 Release Overview, *Nuclear Technology, 180* (2012), 12, pp. 298-315

[12] ***, Reed Robert Burn, Introduction to Nuclear Reactor Operations, Detroit Edison Company, University of Michigan, Ann Arbor, Mich., USA, 1988

[13] ***, US Department of Energy, DOE Fundamentals Handbook, Nuclear Physics and Reactor Theory, DOE-HDBK-1019, 1993

[14] Rabir, M., *et al.*, Modelling the PUSPATI TRIGA Reactor Using MCNP Code, INIS-IAEA, 2012 http://www.iaea.org/inis/collection/NCLCollectionStore/_Public/44/096/44096872.pdf

[15] ***, Techplot 360 (2014) http://www.tecplot.com/products/tecplot-360/

Фаваз АЛРОУМИ, Донгхун КИМ, Рајан СКАУ, Татјана ЈЕВРЕМОВИЋ

КАРАКТЕРИЗАЦИЈА РЕАКТИВНОСТИ КОНТРОЛНИХ ШИПКИ И ОДНОСА МАКСИМАЛНЕ И СРЕДЊЕ СНАГЕ У ГОРИВНИМ ЕЛЕМЕНТИМА У TRIGA MARK I ИСТРАЖИВАЧКОМ РЕАКТОРУ У ЈУТИ

Реактивност три контролне шипке и однос максималне и средње снаге у горивним елементима истраживачког реактора (ТРИГА МАРК, 100 kW) на Универзитету у Јути одређени су на основу AGENT нумеричког система прорачуна и резултати су детаљно приказани у овом раду. Вредности су поређене са MCNP6 и експерименталним вредностима где су такви подаци били доступни. Додатно су анализирани и приказани неутронски мултипликативни фактор, неутронски флукс и неутронске интеракције. AGENT нумерички систем прорачуна реактора је опште-познат и добро евалуиран за разне типове нуклеарних реактора и разне геометријске комплексности реакторских језгара. Из тог разлога AGENT се и користи на Универзитету у Јути као основни нумерички приступ у анализи реакторских параметара. Рачунарско време прорачуна је неупоредиво краће у поређењу са MCNP6, док је одступање од MCNP6 вредности реда величине 0,5 % за неутронски мултипликациони фактор и реактивност реактора, и мање од 10 % када се упореде вредности односа максималне и средње снаге у горивним елементима реакторског језгра. Диференцијална и интегрална реактивност све три горивне шипке добијене прорачунима са AGENT системом су упоредиве са вредностима добијеним коришћењем MCNP6 и теоријским и експерименталним вредностима. Реактивност једне од горивних шипки (регулациона горивна шипка) нешто је већа у прорачунима него што је измерена вредност, док је тотална реактивност добијена AGENT прорачуном у бољем слагању са експерименталном вредношћу него вредност добијена MCNP6 прорачуном.

Кључне речи: AGENT, TRIGA, MCNP6, реактивности контролне шипке, реактивности, критичности, однос максималне и средње снаге